World Academy of Science, Engineering and Technology
International Journal of Geotechnical and Geological Engineering
Vol:2, No:5, 2008

Mixed-Mode Study of Rock Fracture Mechanics by using the Modified Arcan Specimen Test

R. Hasanpour, and N. Choupani

***Abstract*—**This paper studies mixed-mode fracture mechanics in rock based on experimental and numerical analyses. Experiments were performed on sharp-cracked specimens using the modified Arcan specimen test loading device. The modified Arcan specimen test was, in association with a special loading device, an appropriate apparatus for experimental mixed-mode fracture analysis. By varying the loading angle from 0° to 90°, pure mode-I, pure mode-II and a wide range of mixed-mode data were obtained experimentally. Using the finite element results, correction factors applied to the rectangular fracture specimen. By employing experimentally measured critical loads and the aid of the finite element method, mixed-mode fracture toughness for the limestone under consideration determined.

***Keywords*—**Rock Fracture Mechanics, Mixed-mode Loading, Finite Element Analysis, Arcan Test specimen.

I. Introduction

FRACTURE mechanics can be applied to many engineering fields including civil and mining engineering, where drilling, excavation, explosion and cutting of rocks are closely related to the strength, stability and fracture of rock materials and structures. Obviously the principles, methods and techniques of fracture mechanics can play an important role in the analysis, design and construction or production for many rock engineering projects [1-14].

In many situations of rock engineering interest, complex stress states predominate in structures and a potential defect may be shaped so that the failure propensity cannot be resolved by uniaxial stress fields. Induced stress fields are mostly singular and set the upper limit for the strength of structures. Cases when the shear component, i.e. mode II, of the stresses dominates are particularly difficult to assess. In the theoretical analyses of mixed-mode fracture problem, one of the basic assumptions is that the stress field near the crack tip is solely determined by the linear elastic singular solution, i.e. linear elastic fracture mechanics (LEFM) prevails [1, 15].

In this study, a modified version of the Arcan specimen was made for the mixed-mode fracture test of one of type rock specimens, which allows mode-I, mode-II, and almost any combination of mode-I and mode-II loading to be tested with the same test specimen configuration. Therefore, disadvantages presented in the previous mixed-mode toughness test methods can be avoided [15, 16].

This investigation seeks to extend understanding of the rock fracture behaviour of a type of limestone under mixed-mode loading conditions through numerical and experimental methods. Using finite element results, correction factors were applied to the limestone specimen and a fourth order polynomial fit was proposed to evaluate the stress intensity factors of a modified version of the Arcan specimen with a crack subjected to mixed-mode loading conditions. The main objective of this study was to determine the fracture toughness K_{IC} and K_{IIC} for the rock under consideration for a wide range of mixed-mode loading conditions. Another goal was to study the relationship between the stress intensity factors and the fracture toughness. Based on those analyses, a mixed-mode fracture criterion for the limestone specimen has been determined.

II. An Overview of Rock Fracture Mechanics

A. Background Theory

Linear elastic fracture mechanics (LEFM) has been found a useful tool for investigation of cracks in rock materials. The purpose of fracture toughness testing is to determine the value of the critical stress intensity factor, or plane strain fracture toughness K_C. This material property is used to characterize the resistance to fracture in the design of structural members. ASTM standards E 399 [17] and D 5045 [18] give some guidance for plane strain mode-I fracture toughness K_{IC} for metals and plastics. The stress intensity factor K_C at the tip of the pre-crack in a compact tension specimen is given by:

$$K_c = \frac{P_c \sqrt{\pi a}}{wt} f(a/w) \quad (1)$$

where P_c is the fracture load, a is crack length, w is the specimen width, t is the specimen thickness, and $f(a/w)$ is a geometrical factor. Linear elastic fracture mechanics and plan strain conditions are the primary requirements.

The stress intensity factors ahead of the crack tip for a modified version of Arcan specimen were calculated by using the following equations [15, 16, 19-26]:

$$K_{IC} = \frac{P_c \sqrt{\pi a}}{wt} f_1(a/w) \quad (2)$$

R. Hasanpour, Postgraduate Student of Rock Mechanics Engineering, is with Mining Engineering Department, Sahand University of Technology, Tabriz, Iran (e-mail: r_hasanpour@sut.ac.ir).

N. Choupani. Assistanct Professor, is with Mechanical Engineering Department, Sahand University of Technology, Tabriz, Iran (e-mail: Choupani@sut.ac.ir).

$$K_{IIC} = \frac{P_c\sqrt{\pi a}}{wt} f_2(a/w) \quad (3)$$

In turn K_{IC} and K_{IIC} are obtained using geometrical factors $f_1(a/w)$ and $f_2(a/w)$ respectively, which are obtained through finite element analysis of Arcan test specimen.

Also energy release rate for isotropic material with edge crack can be calculated from the following relationships:

$$G_I = \frac{K_I^2}{E}, \qquad G_{II} = \frac{K_{II}^2}{E} \quad \text{(Plane stress)} \quad (4)$$

$$G_I = \frac{(1-\nu^2)K_I^2}{E}, \; G_{II} = \frac{(1-\nu^2)K_{II}^2}{E} \quad \text{(Plane strain)} \quad (5)$$

where E is Young's modulus and ν is Poisson's ratio.

B. FE Analysis of Mixed-mode Fracture

The method used to calculate the stress intensity factor was an interaction J-integral method performed in ABAQUS, and is required to separate the components of the stress intensity factors for a crack under mixed-mode loading in conjunction of finite element analysis. The method is applicable to cracks in isotropic and anisotropic materials. Based on the definition of the J-integral, the interaction integrals J_{int}^{α} can be expressed [27]:

$$J_{\text{int}}^{\alpha} = \lim_{\Gamma \to 0} \int_{\Gamma} n. \left(\sigma : \varepsilon_{aux}^{\alpha} I - \sigma . \left(\frac{\partial u}{\partial x} \right)_{aux}^{\alpha} - \sigma_{aux}^{\alpha} . \frac{\partial u}{\partial x} \right) . q \, d\Gamma \quad (6)$$

Where Γ is an arbitrary contour, $\boldsymbol{q}$ is a unit vector in the virtual crack extension direction, **n** is the outward normal to Γ, σ is the stress tensor and $\boldsymbol{u}$ is the displacement vector, as shown in Fig. 1. The subscript aux represents three auxiliary pure mode-I, mode-II, and mode-III crack-tip fields for α=I, II, III, respectively. The domain form of the interaction J-integral is:

$$J_{\text{int}}^{\alpha} = \int_A \lambda(s) n. \left(\sigma : \varepsilon_{aux}^{\alpha} I - \sigma . \left(\frac{\partial u}{\partial x} \right)_{aux}^{\alpha} - \sigma_{aux}^{\alpha} . \frac{\partial u}{\partial x} \right) . q \, dA \quad (7)$$

Where $\lambda(s)$ virtual crack advance and dA is surface element. In the interaction J-integral method [27] the two-dimensional auxiliary fields are introduced and superposed on the actual fields. By judicious choice of the auxiliary fields, the interaction J-integral can be directly related to the stress intensity factors as:

$$K = 4\pi B . J_{\text{int}} \quad (8)$$

Where B is called the pre-logarithmic energy factor matrix, $J_{\text{int}} = \left[J_{\text{int}}^{I}, J_{\text{int}}^{II}, J_{\text{int}}^{III} \right]^T$ and $K = \left[K_I, K_{II}, K_{III} \right]^T$. In linear elastic fracture mechanics, the J-integral coincides with total energy release rate, $J = G_T = G_I + G_{II} + G_{III}$, where G_I, G_{II} and G_{III} are the energy release rates associated with the mode-I, mode-II and mode-III stress intensity factors, respectively.

Numerical analyses were carried out using the interaction J-integral method. Fig. 2 shows example of the mesh pattern of the specimen, which were performed with *ABAQUS* under a constant load of 1000 N. The entire specimen was modeled using eight node collapsed quadrilateral element and the mesh was refined around crack tip, so that the smallest element size found in the crack tip elements was approximately 0.25 mm. A linear elastic finite element analysis was performed under a plain strain condition using $1/r^{0.5}$ stress field singularity. To obtain a $1/r^{0.5}$ singularity term of the crack tip stress field, the elements around the crack tip were focused on the crack tip and the mid side nodes were moved to a quarter point of each element side.

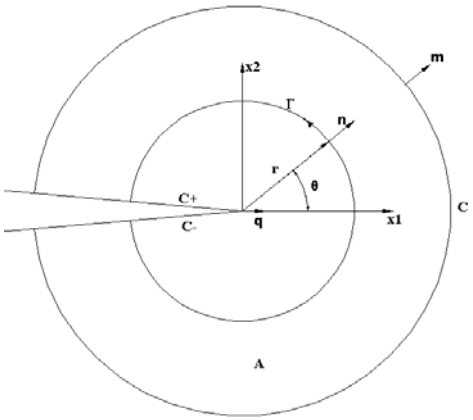

Fig. 1 Contour for evaluation of the J-integral

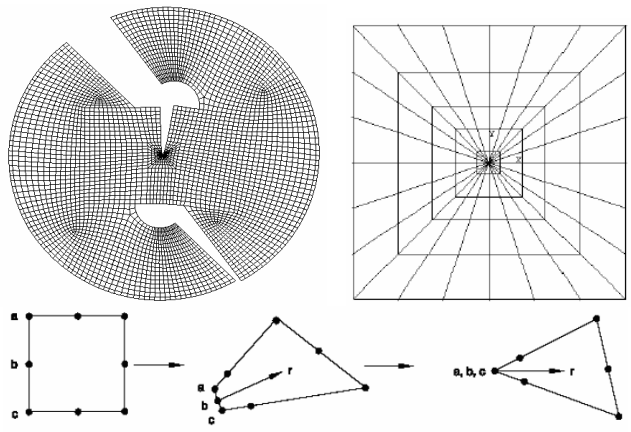

Fig. 2 Finite element mesh pattern of the entire specimen and around the crack-tip of limestone with crack length *a= 30 mm*

III. Rock Material

The examined milky limestone is from a quarry near Khoramabad, Lorestan, Iran. It's related to Asmari formation where the majority of oil reservoirs located there. Also it's widely has been used as building stone. The values of unconfined Young's modulus, *E*, and uniaxial compressive strength, σ_c, of the Khorramabad sandstone are *E=29±5GPa and* σ_c*=105±14MPa*. The average dry density is ρ*=2.3gr/cm*^{3}.

IV. Test Method and Setup

A. Specimen Geometry and Test Rig and Setup

The test specimens were cut from blocks in both the longitudinal and transverse directions to the dimensions of $90\times60\times10$ mm^3. The dimensions of the modified Arcan test specimen used are showed in Fig. 3. Three holes were drilled along the top and bottom edges of the specimen. Sharp crack-shaped notches were made with a thin band saw of 0.8–1mm thickness with *a/w=0.45*. For the testing of the rock specimens in pure mode I, pure mode II and mixed-mode loading conditions, then the crack-tip extended to *a/w=0.5*. A simple and compact fracture mechanics specimen was used for the determination of fracture toughness under mode-I, mode-II and mixed-mode loading conditions. The loading device is simply installed in the universal testing machine and generates accurately repeatable multiaxial loading conditions, Fig. 4.

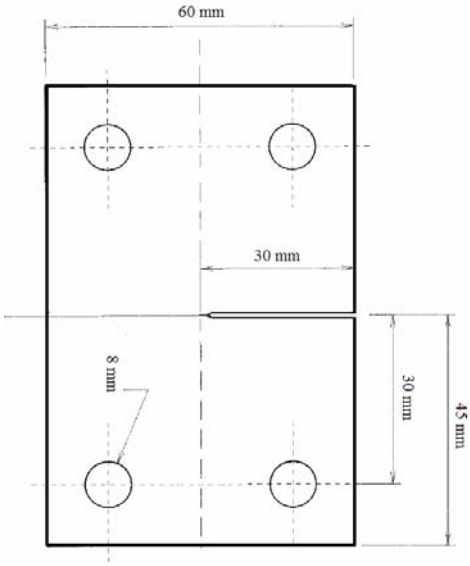

Fig. 3 Modified Arcan test specimen

The tests were displacement-controlled; this was because load-controlled testing was difficult to achieve with the small loads that had to be applied on the specimen. All specimens were tested at the same displacement rate of 0.5mm/minute. Load and displacements were recorded with the built-in load cell during the whole test. All tests were carried out using a kind of universal tension testing machine (UTM). A total of 21 specimens were tested in this survey. Tests were repeated 3 times for mode-I, mode-II, 15°, 30°, 45°, 60° and 75° loading angels.

B. Test Method

From the load-displacement curve, a fracture load P_Q was defined according to the *ASTM Standard E 399* [17]. K_Q was calculated from the following relationship;

$$K_Q = \frac{P_Q\sqrt{\pi a}}{wt} f(a/w) \qquad (9)$$

K_Q value computed from (9) is a valid K_I *or* K_{II} results only if all the validity requirements were met [17]. K_I and K_{II} are obtained using geometrical factors *f (a/w),* i.e. f_I *or* f_{II} respectively in (9). In turn f_I *or,* f_{II} are obtained from a finite element model of the modified Arcan test specimen.

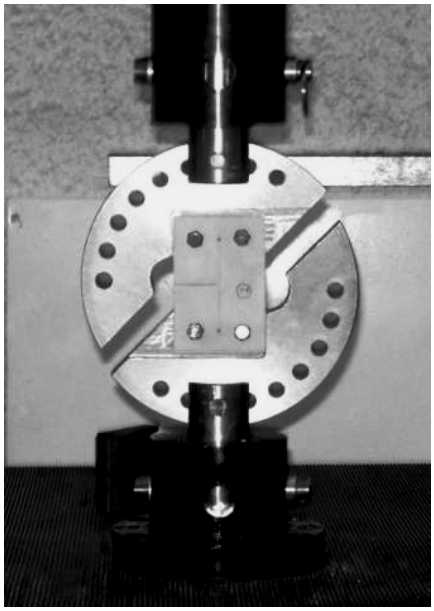

Fig. 4 Geometry of the loading and modified version of Arcan specimen

V. Numerical Results

A. Mixed-Mode Rock Fracture Specimen Calibration

In order to assess geometrical factors or non-dimensional stress intensity factors $f_I(a/w)$ and $f_{II}(a/w)$ for Limestone, the *a/w* ratio was varied between 0.1 and 0.5 at 0.1 intervals and a third order polynomial was fitted through finite element analysis as (Fig. 5):

$$f_I(a/w)(\alpha=0) = 11.836(a/w)^3 - 0.8027(a/w)^2 + 0.31(a/w) + 1.3769$$

$$f_{II}(a/w)(\alpha=90) = 13.387(a/w)^3 - 16.394(a/w)^2 + 7.6616(a/w) - 0.1627$$

Here *a/w* is the crack length ratio, where *a* is the crack length and *w* is the specimen length.

The relationship between the non-dimensional stress intensity factor and the loading angle is shown in Fig. 6. It can be seen that for loading angles $\alpha\leq60^o$, the mode-I fracture is dominant and as the mode-II loading contribution increases, the mode-I stress intensity factor decreases and the mode-II stress intensity factor increases. For $\alpha\geq75^o$ mode-II fracture becomes dominant.

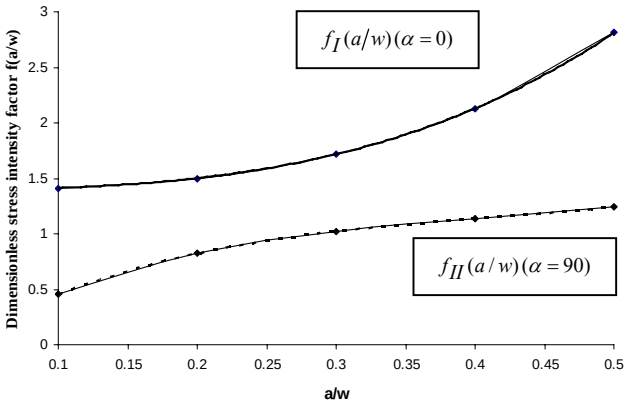

Fig. 5 Non-dimensional stress intensity factors versus crack length of limestone

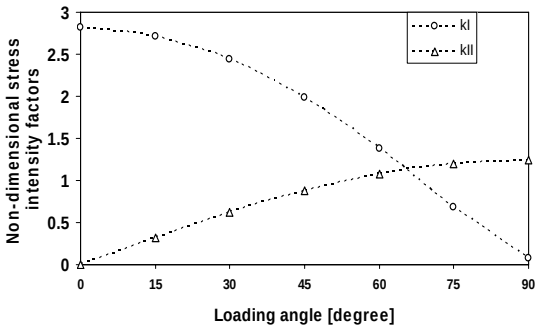

Fig. 6 Non-dimensional stress intensity factors vs. loading angle of limestone for the crack length a= 30 mm

B. Effect of Mixed-mode Conditions on Rock Fracture Characterizations

The strain energy release rates were calculated using Equations 4. The relationship between the mixed-mode ratios of strain energy release rates and the loading angles α is shown in Fig. 7. For loading angles close to pure mode-I loading, very high ratios of mode-I to mode-II are dominant. The ratios of strain energy release rates close to pure mode-II loading exhibit the opposite trend. As expected, it is confirmed that by varying the loading angle of the Arcan specimen, pure mode-I, pure mode-II and a wide range of mixed-mode loading conditions can be created and tested.

In Fig. 8, strain energy release rates G_I and G_{II} obtained by Equations 4 and the total strain energy release rate obtained by $G_T = G_I + G_{II}$ are compared for a constant value of the load. It is seen that for loading angles $\alpha \leq 60^o$ the mode-I strain energy release rate is maximum and as loading angle increases, G_I decreases and G_{II} increases. For $\alpha \geq 75^o$ mode-II fracture becomes dominant. The total strain energy release rate under mixed-mode loading condition decreases with the loading angle. Therefore, the increase of the mode-II loading contribution leads to a reduction in the total strain energy release rate.

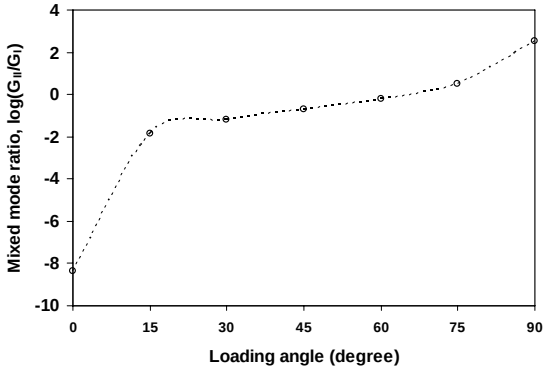

Fig. 7 The ratio of mode-II to mode-I, G_{II}/G_I (in logarithmic scale), versus loading angle (α) for limestone with crack length *a=30 mm*

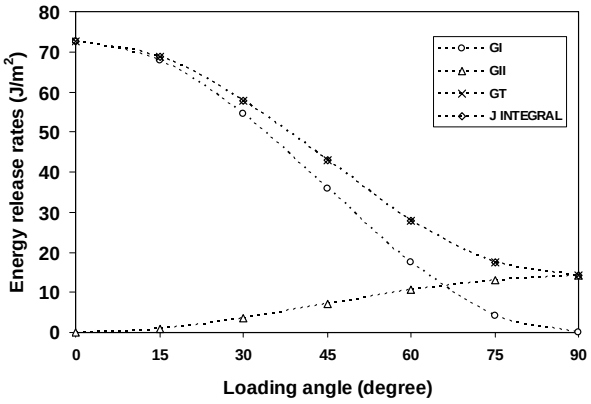

Fig. 8 Strain energy release rates G_I, G_{II}, $G_T=G_I+G_{II}$ versus loading angle, α for limestone with crack length *a*= 30 mm

VI. Experimental Results

A. Rock Fracture Mechanics Tests

Fracture tests were carried out using a kind of universal tension testing machine (UTM). All tests were conducted by controlling the constant displacement rate of 0.5mm/min in order to reduce dynamical effects and the fracture loads and displacements were recorded.

Tests were repeated 3 times for mode-I, mode-II, 15°, 30°, 45°, 60° and 75° loading angels. A total of 21 specimens were tested in this survey. The load-displacement curves generated by the test machine were used to determine maximum load and displacement. Fig. 9 shows the typical load-displacement curve of Limestone for pure mode-I. The average values of critical fracture loads were used to determine the critical mixed-mode stress intensity factors and strain energy release rates data. Also the fracture was found to be completely brittle with the load-displacement curves.

TABLE I
AVERAGE CRITICAL STRESS INTENSITY FACTORS $(K)_C$ [MPA.M$^{1/2}$] FOR LIMESTONE WITH CRACK LENGTH 30 MM

loading angle	0°	15°	30°	45°	60°	75°	90°
$(K_I)_C$ [Mpa.m$^{1/2}$]	0.94	0.92	0.84	0.73	0.58	0.34	-
$(K_{II})_C$ [Mpa.m$^{1/2}$]	-	0.11	0.21	0.32	0.45	0.61	0.70

TABLE II
AVERAGE CRITICAL ENERGY RELEASE RATE $(G)_C$ [J/M^2] FOR LIMESTONE WITH CRACK LENGTH 30 MM

loading angle	0°	15°	30°	45°	60°	75°	90°
$(G_I)_C$ [j/m^2]	309.6	294.3	249.4	188.9	119.4	41.5	-
$(G_{II})_C$ [j/m^2]	-	4.1	16.1	36.9	72.4	129.7	169.8
G_T [j/m^2]	309.6	298.4	265.5	225.8	191.8	171.2	169.8

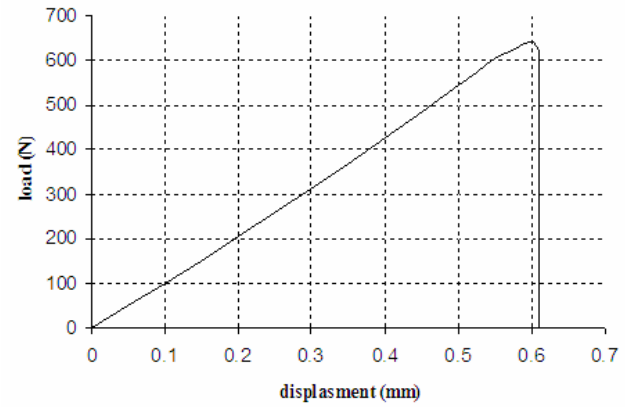

Fig. 9 Typical Load-Displacement curve of Limestone

B. Mixed-Mode Rock Fracture Toughness

Rock fracture toughness was determined experimentally with the modified version of the Arcan specimen under different mixed-mode loading conditions. The average values of mixed-mode critical stress intensity factors for Limestone are summarized in Table I. $(K_I)_C$ remains almost unchanged until α=30° and then decreases and $(K_{II})_C$ increases as the mode-II loading contribution, i.e. as α increases from 0° to 90°. It is seen that for loading angles α≤60° the mode-I contribution is greater than that of mode-II and the opening-mode fracture becomes dominant. For loading angles α≥75° there is an opposite trend and the shearing-mode fracture becomes dominant. From Table I, It can be seen that the shearing-mode (α=90°) fracture toughness is smaller than the opening-mode (α=0°) fracture toughness. This means that the cracked specimen is tougher in tensile loading conditions and weaker in shear loading conditions.

Also Fracture toughness measurements for the modified Arcan specimen under pure mode-I loading show the average fracture toughness of $K_{IC}=(K_I)_C=0.94$ [MPa.m$^{1/2}$] for Limestone with crack length 30mm. For pure mode-II loading using modified Arcan specimen, the average fracture toughness for Limestone is found $K_{IIC}=(K_{II})_C=0.70$ [MPa.m$^{1/2}$].

The calculated critical strain energy release rate values $(G_I)_C$ and $(G_{II})_C$ using experimental data under various loading conditions are summarized in Table II. $(G_I)_C$ decreases while $(G_{II})_C$ increases with an increase in mode-II loading contribution. The opening-mode and shearing-mode critical strain energy release rates were found approximately 309.6 J/m^2 and 169.8 J/m^2, respectively. Table II also shows the total strain energy release rate, $(G_T)_C=(G_I)_C+(G_{II})_C$ under various loading conditions, which decreases with the loading angle. Therefore, it is confirmed that the maximum fracture toughness occurs at mode-I loading condition.

Also pure mode-I and pure mode-II fracture toughness of Limestone specimens were approximately $G_{IC}=(G_I)_C=$ 309.6 J/m^2 and $G_{IIC}=(G_{II})_C=$ 169.8 J/m^2, respectively. It can be seen that G_{IIC} is smaller than G_{IC}, indicating that the cracked specimen is tougher in mode-I and weaker in mode-II loading conditions.

VII. CONCLUSION AND SUMMARY

In this paper the mixed-mode fracture behaviour of Limestone specimens was investigated based on experimental and numerical analyses. A modified version of the Arcan specimen was employed to conduct a mixed-mode test using the special test loading device. The full range of mixed-mode loading conditions including pure mode-I and pure mode-II loading can be created and tested. It is a simple test procedure, clamping/unclamping the specimens is easy to achieve and only one type of specimen is required to generate all loading conditions.

The finite element results indicate that for loading angles close to pure mode-II loading, a high ratio of mode-II to mode-I fracture is dominant and there is an opposite trend for loading angles close to pure mode-I loading. It confirms that by varying the loading angle of Arcan specimen pure mode-I, pure mode-II and a wide range of mixed-mode loading conditions can be created and tested. Also, numerical results confirm that the increase of the mode-II loading contribution leads to an increase of fracture resistance in the Limestone (i.e., a reduction in the total strain energy release rate) and the increase of the crack length leads to a reduction of fracture resistance in the Limestone (i.e., an increase in the total strain energy release rate).

The fracture toughness was determined experimentally with the modified version of the Arcan specimen under different mixed-mode loading conditions. The results indicated that the cracked specimen is weaker in shear loading conditions and tougher in tensile loading condition.

REFERENCES

[1] L. Lim, I. W. Johnston, S. K. Choi, J. N. Boland, "Fracture Testing of a Soft Rock with Semi-circular Specimens Under Three-point Bending.

Part 2--Mixed-mode", Int. J. Rock Mech. Min. Sci. & Geomech. Vol. 31, No. 3, pp. 199-212, 1994.
[2] Y. Nara, K. Kaneko, "Sub-critical crack growth in anisotropic rock" International Journal of Rock Mechanics & Mining Sciences vol. 43, p. 437–453, (2006).
[3] T. Backers, S. Stanchits, G. Dresen, "Tensile fracture propagation and acoustic emission activity in sandstone: The effect of loading rate" International Journal of Rock Mechanics & Mining Sciences vol. 42, p. 1094–1101, (2005).
[4] Y. Nara, K. Kaneko, "Study of subcritical crack growth in Andesite using the Double Torsion test" International Journal of Rock Mechanics & Mining Sciences vol. 42, p.521–530, (2005).
[5] Feng Chen, Ping Cao, Q.H. Rao, C.D. Ma, Z.Q. Sun, "A mode II fracture analysis of double edge cracked Brazilian disk using the weight function method" International Journal of Rock Mechanics & Mining Sciences vol. 42, p.461–465, (2005).
[6] M.H.B. Nasseri, B. Mohanty, P.-Y. F. Robin, "Characterization of microstructures and fracture toughness in five granitic rocks" International Journal of Rock Mechanics & Mining Sciences vol. 42, p.450–460, (2005).
[7] J.G. Donovan, M.G. Karfakis, "Adaptation of a simple wedge test for the rapid determination of mode I fracture toughness and the assessment of relative fracture resistance", International Journal of Rock Mechanics & Mining Sciences vol. 41, p.695–701, (2004).
[8] Q.Z. Wang, X.M. Jia, L.Z. Wu, "Wide-range stress intensity factors for the ISRM suggested method using CCNBD specimens for rock fracture toughness tests" International Journal of Rock Mechanics & Mining Sciences vol. 41, p. 709–716, (2004).
[9] Q.Z. Wang, L.Z. Wu, "The flattened Brazilian disc specimen used for determining elastic modulus, tensile strength and fracture toughness of brittle rocks: experimental results", International Journal of Rock Mechanics & Mining Sciences vol. 41, p. 357–358, (2004).
[10] H.Y. Liu, S.Q. Kou, P.-A. Lindqvist, C.A. Tang, "Numerical simulation of shear fracture (Mode II) in heterogeneous brittle rock", International Journal of Rock Mechanics & Mining Sciences, vol. 41, p. 355, (2004).
[11] Jeoungseok Yoon, Seokwon Jeon, "Experimental verification of a (Punch through Shear) PTS Mode II test for rock", International Journal of Rock Mechanics & Mining Sciences vol. 41, p. 353–354, (2004).
[12] Q.Z. Wang, X.M. Jia, S.Q. Kou, Z.X. Zhang, P. -A. Lindqvist, "More accurate stress intensity factor derived by finite element analysis for the ISRM suggested rock fracture toughness specimen—CCNBD" International Journal of Rock Mechanics & Mining Sciences vol. 40, p. 233–241, (2003).
[13] T. Backers, O. Stephansson, E. Rybacki "Rock fracture toughness testing in Mode II—punch through shear test", International Journal of Rock Mechanics & Mining Sciences vol. 39, p. 755–769, (2002).
[14] Z.X. Zhang, "An empirical relation between mode I fracture toughness and the tensile strength of rock" International Journal of Rock Mechanics & Mining Sciences vol. 39 p. 401–406 (2002).
[15] Choupani, N. "Experimental and Numerical Investigation of the Mixed-Mode Delamination in Arcan Laminated Specimens", International Journal of Materials Science & Engineering, in press.
[16] P.M. Noury, R.A. Shenoi and I. Sinclair, "On mixed-mode fracture of PVC foam", International Journal of Fracture vol. 92, p. 131–151, 1998.
[17] ASTM E399, Standard Test Method for Plane Strain Fracture Toughness and Strain Energy Release Rate of Metalic Materials: Annual Book of ASTM Standards, 1983.
[18] ASTM D5045, Standard Test Method for Plane Strain Fracture Toughness and Strain Energy Release Rate of Plastic Materials: Annual Book of ASTM Standards, 1995.
[19] R. A. Jurf, R. B. Pipes, "Interlaminar Fracture of Composite Materials", J. Composite Materials, vol. 16, p. 386-394, 1982.
[20] M. Arcan, Z. Hashin, and A. Voloshin, "A Method to Produce Plane-Stress States with Applications to Fiber-Reinforced Materials", Experimental Mechanics, vol. 18, p. 141-6, 1978.
[21] S. H. Yoon and C. S. Hong, "Interlaminar Fracture Toughness of Graphite/Epoxy Composite under Mixed-Mode Deformations", Experimental Mechanics, vol. 30(3), p. 234-239, 1990.
[22] L. Banks-Sills, M. Arcan, and Y. Bortman, "A Mixed Mode Fracture Specimen for Mode II Dominant Deformation", Engineering Fracture Mechanics, vol. 20(1), p. 145-157, 1984.
[23] K. J. Miller and D. L. McDowell, "Mixed-Mode Crack Behavior", West Conshohocken, Penn: ASTM, 1999.
[24] H. P. Rossmanith and K. J. Miller, "Mixed-Mode Fatigue and Fracture": Papers Presented at the International Conference on Mixed-Mode Fracture and Fatigue Held at the Technical University of Vienna, Austria. London: European Structural Integrity Society: Mechanical Engineering Publications, 1993.
[25] E. E. Gdoutos, Problems of Mixed Mode Crack Propagation. Boston; Hingham, MA, USA: M. Nijhoff ; Distributors for the U.S. and Canada, Kluwer Boston, 1984.
[26] E. E. Gdoutos, D. A. Zacharopoulos, and E. I. Meletis, "Mixed-Mode Crack Growth in Anisotropic Media", Engineering Fracture Mechanics, vol. 34(2), p. 337-346, 1989.
[27] Habbit, Karlsson, and Sorensen, "ABAQUS User's Manual Version 6.2.4," 2001.